International Journal of Nanoelectronics and Materials
Volume 14 (Special Issue) August 2021 [263-274]

Effects of Total Disc Replacement on Range of Motion and Facet Stress in Lumbar Spine Using a Finite Element Analysis

M.A. Suarin[1,2], M.J.A. Latif[1,3*], M.S. Zakaria[1], M.N. Harun[4] and H.Q. Nguyen[5]

[1]Fakulti Kejuruteraan Mekanikal, Universiti Teknikal Malaysia Melaka, Hang Tuah Jaya, 76100 Durian Tunggal, Melaka, Malaysia.

[2]Jabatan Kejuruteraan Mekanikal, Politeknik Ungku Omar, Jalan Raja Musa Mahadi, 31400 Ipoh, Perak, Malaysia.

[3]Advanced Manufacturing Centre, Universiti Teknikal Malaysia Melaka, Hang Tuah Jaya, 76100 Durian Tunggal, Melaka, Malaysia.

[4]Faculty of Mechanical Engineering, Universiti Teknologi Malaysia, 81310 Skudai, Johor, Malaysia.

[5]Institute of Engineering and Technology, Thu Dau Mot University, Thu Dau Mot City, Binh Duong Province, Vietnam.

ABSTRACT

The focus of this study was to investigate the effects total disc replacement (TDR) on the range of motion (ROM) and facet joint stress at the lumbar spine region. A three-dimensional (3D) finite element model of the osseoligamentous lumbar spine was developed and subjected to the moment load in flexion, extension, left bending, and right torsion. The findings of this study indicated that the implanted spine with Prodisc-L caused an increase in ROM during flexion-extension motion and left bending motion ranged from 1% to 5%. However, ROM decreased during torsion motion by 7% after TDR. Meanwhile, the facet stress values increased at the treated level of L4L5 after Prodisc-L implantation ranging from 12% to 27% of differences in all spine motion. But, decreasing values was observed in most of the adjacent level for both left and right facets. In brief, this phenomena could be one of the potential causes of early facet arthrosis, facet degeneration, and lower back pain in the immediate future.

Keywords: Facet stress, finite element method, lumbar spine, range of motion, total disc replacement.

1. INTRODUCTION

Total discs replacement (TDR) is an alternative of common fusion technique which is to replace the degenerated disc with artificial discs [1], [2]. This is to preserve the spine motion and reduce back pain particularly caused by degenerative disc disease [3]. Various artificial discs have been developed in TDR treatment [2], [4]. The bearing systems designed of the artificial discs includes Metal-on-Polymer (MoP) has difference purposes and advantages. The ball and socket geometry's implants with bearing system of MoP such as Prodisc and Maverick have been widely used in order to preserved spinal motion [5]. The implementation of ball and socket geometry's artificial disc, such as Prodisc L, has been shown successfully as the most preferred prosthesis it was recognized by the Food and Drug Administration(FDA) [3], [6], [7]. Nevertheless, clinical complications have also been reported.

Several aspects, including the surgical procedure and prosthesis placement, have led to complications regarding TDR [8]. The primary concern was the removal of the anterior longitudinal ligament and annulus fibrosus during the surgical procedure, which may affect

ROM because these tissues were essential in preserving the stability of spinal segment motion [8]–[10]. The ball-and-socket implants were reported to cause extreme joint movement at surgical level, resulting in unnecessary facet contact forces [8], [10], [11]. The facet joints may develop severe degeneration due to it high mobility level and the heavy stress affecting the facet joints which could contribute to facet joint osteoarthritis that lead to reoccurance of back pain [12].

Though some biomechanical effects have been identified in TDR of the lumbar spine, the influence of TDR on ROM and facet joint have yet to be studied in depth. Therefore, this study aimed to investigate the effects of TDR prosthesis on the spinal facet joint on the ROM and facet stress at the lumbar spine region in flexion, extension, left bending, and right torsion motions using finite element (FE) method.

2. MATERIALS AND METHODS

2.1 Finite Element Modeling

The computed tomography (CT) scan data of human lumbar spine was obtained from Hospital Tengku Ampuan Afzan, Kuantan, Pahang, Malaysia based on a healthy 21-year-old male volunteer with 173 cm height and 70 kg weight. The data segmentation process was performed using Mimics 14.0 software (Materialise, Leuven, Belgium) to develop 3D model of the lumbar spine as shown in Figure 1. For the intervertebral disc (IVD), the volumetric ratio between the annulus fibrosus and the nucleus pulposus was set to be 3:7 [13], [14]. The annulus fibers were constructed using 3D two-nodes truss element [15]. The cartilage tissue was extruded 2 mm thickness from the articular facet joint [16], [17]. The initial gap between the cartilage tissues was assumed to be 0.5 mm [15], [16].

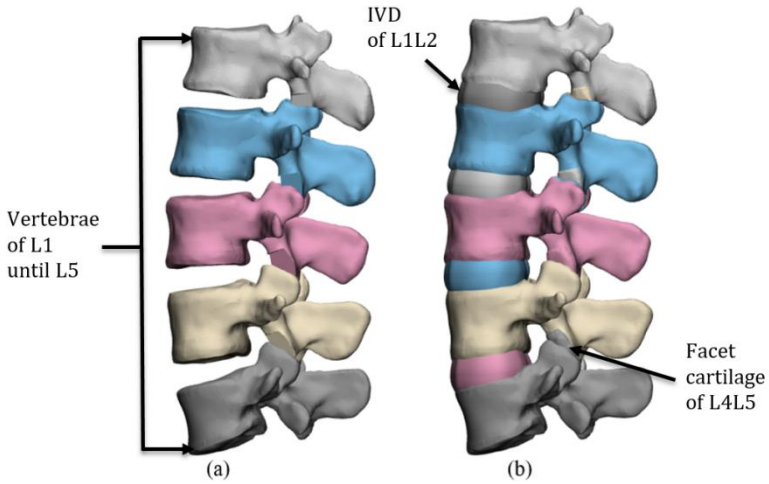

Figure 1. 3D model of lumbar vertebrae. (a) 3D model generated from CT scan without soft tissues (b) 3D model completed with soft tissues.

All the ligaments were modeled as two-node truss elements, which were only active under the presence of tension [15], [18]. The overall meshing process of the 3D model was carried out using 3-Matic Research 13.0 software (Materialise, Leuven, Belgium). The standard tessellation language (STL) surfaces files of vertebrae, intervertebral discs, nucleus, and facet cartilages were converted into solid linear first-order tetrahedral elements. The Mooney-Rivlin constitutive model was used to represent the incompressible and hyperelastic characteristics of the annulus fibrosus and nucleus [18]. Meanwhile, the facet cartilages were modeled as a

smooth surface to simulate the synovial fluid in the facet cartilage where the original gap between the cartilage layers was 0.5 mm with linear elastic and isotropic behaviors [15], [16]. The seven spinal ligaments were represented by tension-only truss element and nonlinear material properties of non-linear stress-strain curve [15], [16].

The 3D geometrical model of Prodisc-L artificial disc was constructed based on the dimension obtained from the Manual of Prodisc-L: Surgical Technique distributed by DePuy Synthes Spine (Synthes Spine, West Chester, NY, USA). The 3D model was then converted into a solid tetrahedral FE model using automatic solid meshing function in 3-Matic Research 13.0 software as shown in Figure 2. The superior and inferior materials of the prosthesis were made of Cobalt-Chromium-Molybdenum (CoCrMo) alloy [5], [19]. The implantation was performed for single-level implantation at L4-L5 vertebral segment as shown in Figure 3. It is the most frequent vertebral segment at the lumbar spine region treated using TDR technique because its most heavily burdened spinal segment [16]. The prosthesis was implanted using an anterior surgical approach where the ALL and nucleus of L4-L5 were completely removed and lateral annulus was preserved according to the size of the artificial disc.

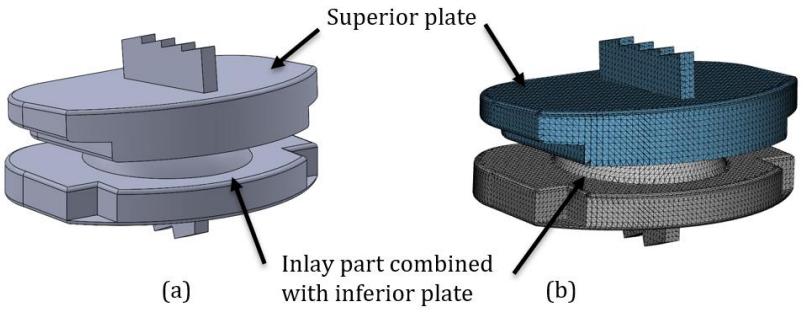

Figure 2. Prodisc-L® prosthesis (a) 3D geometrical model and (b) FE model.

2.2 Finite Element Analysis

The FE analysis was carried out using Abaqus/ CAE 6.14-1 software (Dassault Systemes Simulia Corp., RI, USA). The FE model was simulated in three different planar motions which are flexion-extension, bending, and torsion. The loading was applied based on the motions where 8 Nm of flexion moment, 6 Nm of extension moment, 6 Nm of lateral bending moment, and 4 Nm of torsion moment were applied separately to the lumbar FE model as shown in Figure 3. Each of the moment load was added to the compressive follower loads of 650 N, which represented the upper bodyweights of normal BMI. The follower load of the FE model was calculated based on 65% of the upper bodyweight with an additional 200 N of the local muscles [20], [21].

The boundary condition was set in a fixed displacement at the inferior surface of the L5 vertebral body as shown in Figure 3. The contact surfaces of the FE model such as the vertebral body, nucleus and intervertebral disc, were perfectly placed and held together using tie constraint, as well as the contact between the ligaments and the vertebral body. Meanwhile, the contact between the inferior and superior facets was modelled as surface-to-surface contact with normal behavior of 200 N/mm contact stiffness and frictionless of tangential behavior [15]. The material properties assigned in the FE model are shown in Table 1.

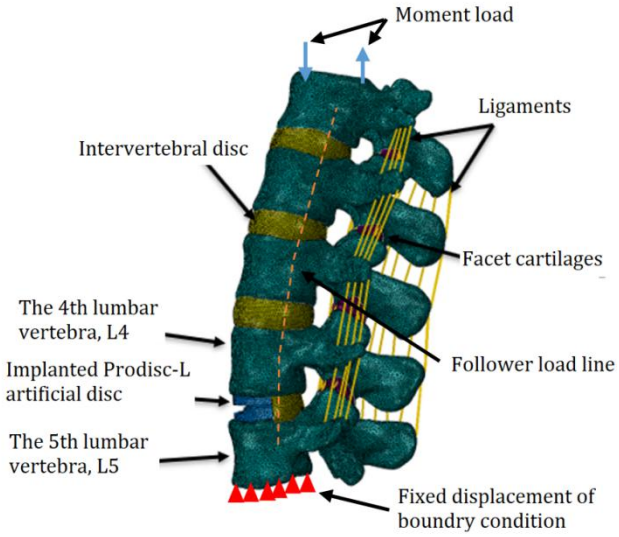

Figure 3. Finite element model of osseoligamentous lumbar spine.

Table 1 Material properties of the osseoligamentous lumbar spine model [16]

Element Set	Type of element	Material Properties
Cortical bone	3D linear tetrahedron	E = 12,000 MPa, v = 0.3
Cancellous bone	3D linear tetrahedron	E = 100 MPa, v = 0.2
Facet cartilage	3D linear tetrahedron	E = 35MPa, v = 0.4
Nucleus pulposus	3D linear hybrid tetrahedron	Mooney-Rivlin: C1 = 0.12, C2 = 0.03
Annulus fibrosus	3D linear hybrid tetrahedron	Mooney-Rivlin: C1 = 0.18, C2 = 0.045
PLL	3D truss.	E = 10.0 MPa (ε<11%), E = 20 MPa (ε >11%)
ALL	3D truss.	E = 7.8 MPa (ε <12%), E = 20 MPa (ε >12%)
LF	3D truss.	E = 15.0 MPa (ε <6.2%), E = 19.5 MPa (ε >6.2%)
CL	3D truss.	E = 7.5 MPa (ε <25%), E = 32.9 MPa (ε >25%)
ITL	3D truss.	E = 10.0 MPa (ε <18%), E = 58.7 MPa (ε >18%)
ISL	3D truss.	E = 10.0 MPa (ε <14%), E = 11.6 MPa (ε >14%)
SSL	3D truss.	E = 8.0 MPa (ε <20%), E = 15.0 MPa (ε >20%)
Prodisc-L	3D linear tetrahedron	E = 210,000 Mpa, v = 0.3

E: Young's modulus; ν: Poisson's ratio; ε: Strain; C1 and C2: Material constants characterise the deviatoric deformation of a material

3. RESULTS AND DISCUSSIONS

3.1 Verification of FE Model

In order to verify the osseoligamentous FE model of L1-L5 lumbar spines, the ROM obtained from the present study was compared with previous in vitro studies [22], [23]. Each level of vertebral segment in flexion-extension, lateral bending, and axial rotation were verified and compared with another previous *in vitro* experiments. The FE model was subjected to 8 Nm of moment load for flexion motion and 6 Nm of moment load for extension motion. Figure 4 (a) shows the comparison of the flexion-extension motion for each level of vertebrae with previous *in vitro* studies [22], [23]. The present FE model produced the ROM within the range of the previous *in vitro* studies, which was between 0.8% and 39%. Lower percentage differences of the ROM were found from vertebral segments L1-L2 to L4-L5 between 0.8% to 15%. However, the percentage difference of L1-L5 was observed to be only 1% to 2% when compared with both in vitro experiments [22], [23]. For the FE model with lateral bending motion under 6 Nm of moment load, the range of ROM were also within the range with the previous *in vitro* experiments as shown in Figure 4(b). Generally, the ROM of L1-L5 for bending motion was within the range with both previous *in vitro* studies where the differences were between 1.8% and 15% [22], [23].

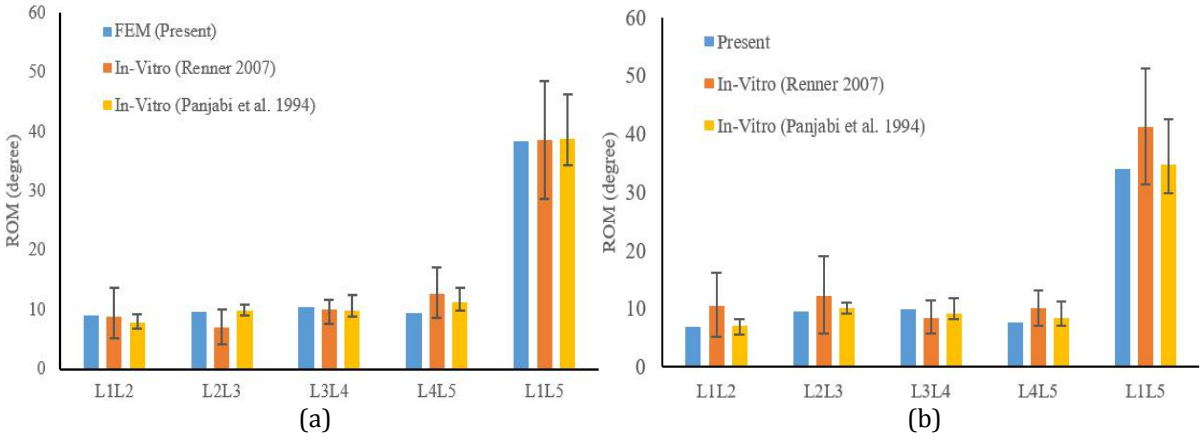

Figure 4. ROM of the lumbar spine in (a) flexion-extension motion, (b) lateral bending.

Meanwhile in torsion motion, the ROM generated from the present FE model was within the range despite the noticeable outcomes from both of the previous *in vitro* studies as shown in Figure 5(a). The IVD was verified by comparing the disc displacement of all IVD segments subjected to 1200 N of compression follower load. Figure 5(b) shows the comparison of the present FE model with the previous *in vitro* and FE studies. From the present study, the disc compressions at the IVD level of L1-L2, L2-L3, and L3-L4 were higher than that of previous *in vitro* study except for L4-L5. The highest percentage difference of 48% was found at the IVD level of L2-L3. The large percentage difference was due to the compression load caused by a small change of the path position [24]. However, the present findings were still within the range and comparable with the previous *in vitro* and FE studies.

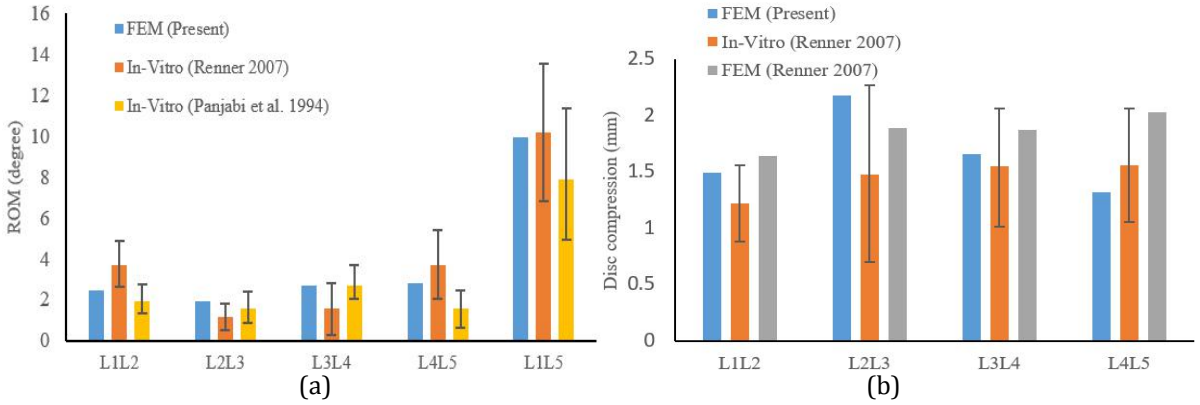

Figure 5. (a) ROM of the lumbar spine in torsion, (b) Disc compression of the lumbar spine.

Based on the results, the present FE model can replicate the physiological *in vitro* study of the lumbar spine since all of the data obtained by the present FE model were in the acceptable range reported by the previous *in vitro* studies. Moreover, the present FE model also capable to produce relevant and reliable findings for the investigation of the biomechanical behaviour of the human lumbar spine.

3.2 Effects of Total Disc Replacement on ROM of Lumbar Spine

The intact and implanted FE models were subjected to 8 Nm flexion and 6 Nm extension moments, along with 650 N follower load. The comparison of ROM between intact and implanted lumbar spine in flexion and extension motion was shown in Figure 6 (a). The highest ROM was observed at L2L3 for intact and implanted lumbar spine were 9.7° and 8.7°, respectively. A slight decreasing trend of ROM for implanted lumbar spine was found at L1L2, L2L3 and L3L4 in a range of 3% untill 19%. However, implanted ROM at L4L5 increased by 40% compared to intact lumbar spine. This result was also observed in clinical studies which an increment of ROM at the treated level after TDR ranged between 23% to 44% [8], [25], [26]. This is due to the resection of ALL at the treated level during TDR surgery, which supposed to stabilize the lumbar spine particularly flexion and extension motions [27], [28]. Generally, the ROM for implanted L1L5 lumbar spine increased by 5% after TDR, which was at 36.43°. Similar finding was reported that TDR had increased the ROM in flexion and extension of lumbar spine, L1L5 in raging between 3% until 25% based on the load applied [29].

A similar trend was observed in the lateral bending subjected to 6 Nm of the moment for implanted lumbar spine compared to intact lumbar as shown in Figure 6(b). The ROM was decreased at L1L2, L2L3 and L3L4 between 9% to 15%. Meanwhile, the highest percentage difference of ROM after TDR was observed at L4L5 with 35% which was lesser than percentage difference of ROM after TDR in flexion-extension at the same level. However, the total ROM for the whole lumbar spine, L1L5 was just 1% increase in percentage difference compared to the intact model. This result was in agreement with the previous in vitro studies that demonstrated ROM of lateral bending movement after TDR was generally maintained or slight increased, which depended on the prosthesis design and position [30]–[32].

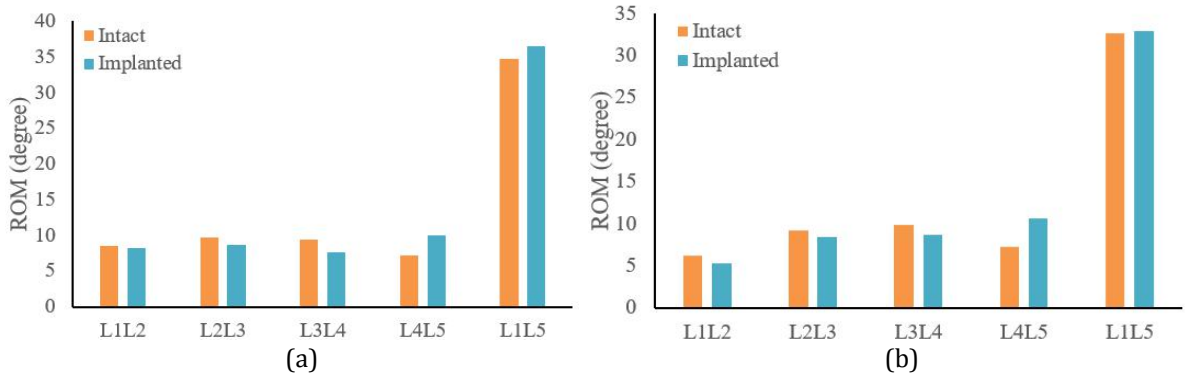

Figure 6. ROM of intact and implanted lumbar spine in (a) flexion-extension loading direction, (b) bending loading direction.

Figure 7 shows the comparison of ROM between the intact and implanted lumbar models subjected to 4 Nm of moment at right torsion. The highest ROM was found at L2L3 for both intact and implanted lumbar spine, which were 3.14° and 3.09°, respectively. A different trend of ROM was observed in the torsion motion for intact and implanted lumbar spine, ROM at L1L2, L2L3 and L3L4 of the implanted model decreased in ranged 5% to 19%. The ROM of L4L5 shows similar trend like others spine motion, which was increased by slight percentage difference of 0.7%. The result was in agreement with previous in-vitro study using seven cadaveric lumbar spines where at the treated level of TDR, there was an increment ranging from 1% to 4.5% of difference, while at the adjacent level, there was a decreasing percentage difference of almost 20% [32]. This is due to the design of the artificial disc used in the present study which is unconstrained ball and socket, as it caused vertebral rotation occurs without much constraint on the axial and other anatomical planes [4], [31].

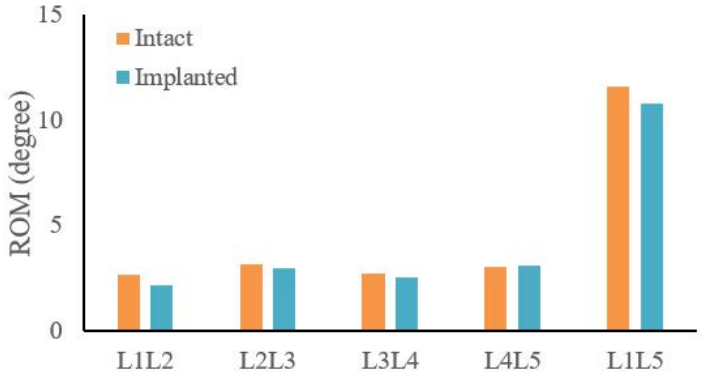

Figure 7. ROM of intact and implanted lumbar spine in clockwise right torsion loading direction.

The findings of this study indicated that the implanted spine with Prodisc-L caused a significant increase in ROM during flexion-extension motion and left bending motion ranged from 1% to 5%. The surgery procedure of TDR also played an essential role in contributing to the change of ROM. Hence, the TDR implant procedure is performed by removing the anterior longitudinal ligament (ALL) of the damaged disc level in order to position the artificial disc between the vertebral body. Lumbar TDR procedure is necessarily compromises the ALL and the annulus fibrosus, giving rise to concerns regarding the possibility of rotational instability [26]. Thus, the natural stiffness of this area may affect ROM after TDR, especially at the treated level [33].

3.3 Effects of Total Disc Replacement on Facet Stress

Figure 8(a) shows the comparison of facet stress in flexion motion for intact and implanted lumbar spine. Flexion motion of the lumbar spine did not produce much stress in the facet due to the rotation of the lumbar caused the facet to move away from each other. Only the left facet of L1L2 and L2L3 displayed a slight sign of facet stress. After TDR, facet stress increased with ranging of 45% to 50% of the percentage difference for both levels of facet.

Figure 8(b) shows the comparison of facet stress for intact and implanted Prodisc-L for the left and right facets in the extension motion. Most of the facet stress at the left side was shows an increasing trend except at L3L4. In contrast, at the right side of the facet, displayed decreasing trend of facet stress after TDR except at L4L5, where the treated level shows increasing trend for both side of facet. The highest stress results for extension motion occurs at L1L2 of left facet, which are 3.24 MPa for intact and 3.51 MPa for implanted lumbar spine, which increased by 8.3%. The highest increased different percentage was observed at the treated level, where the facet stress shows a significant increase of 27% for the left facet and 15% of the right facet. The complex geometry of the spine and the asymmetry of the compressive load subjected to the spine may affected the transmitted load between the superior and inferior facet contact consiquently could cause the facet stress values [34]. However, the trend difference of the changed conditions was reliable in the study as the perentage differences ranged from 5% to 30% [33].

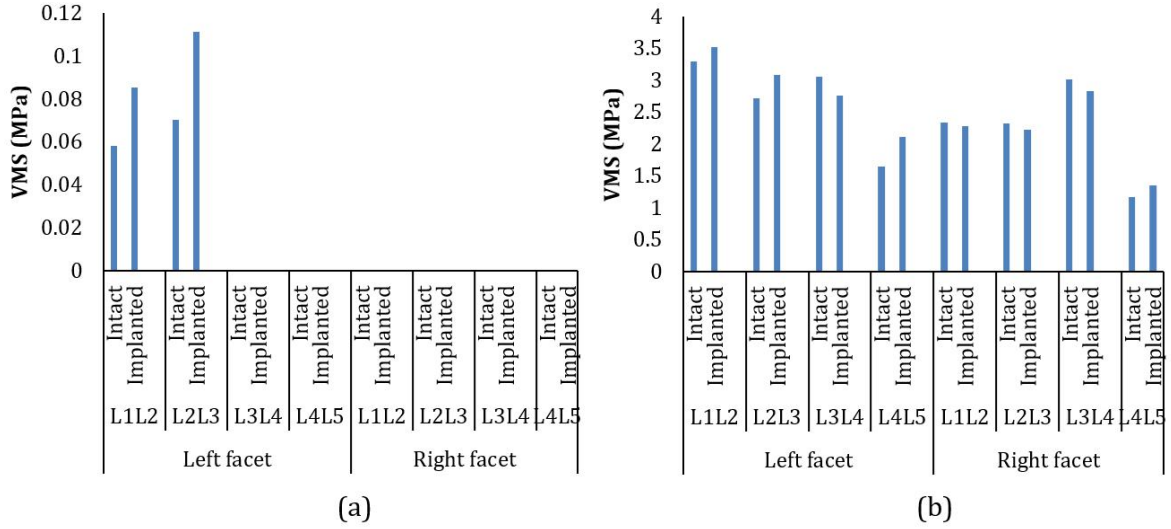

Figure 8. Facet stresses in the lumbar spine between intact and implanted lumbar spine in (a) flexion motion, (b) extension motion.

The results show in Figure 9(a) indicates that the increasing facet stress not only at treated level but also at L2L3 and L3L4 of right facet. The decreasing trend of facet stress was observed on the left facet with 22% of L2L3 and 9% of L3L4 and the right facet with 6.9% of L1L2. Meanwhile, increasing trend of facet stress was observed on both left and right facet of L4L5. The facet stress at L4L5 of left facet generated the highest stress value of 3.8 MPa during left bending motion. The present study is in agreement with those previous studies for implanted lumbar during left bending motion. In previous computational and in vitro studies reported that the facet contact stress increased after TDR at bending and axial rotation motions [10], [34], [35].

Figure 9(b) shows the comparison of facet stress between intact and implanted lumbar spine at the left and right facet in right torsion motion. The torsion motion recorded the highest value of facet stress that reached 4.3 MPa at the treated level of the implanted model, which increased by

27% from the intact model. Meanwhile, others level of facet displayed decreased trend after TDR ranging from 4.5% to 5.7%. Similar finding was also found in previous study where significant increase in facet stress at the level of TDR was demonstrated with side bending and axial torsion [34].

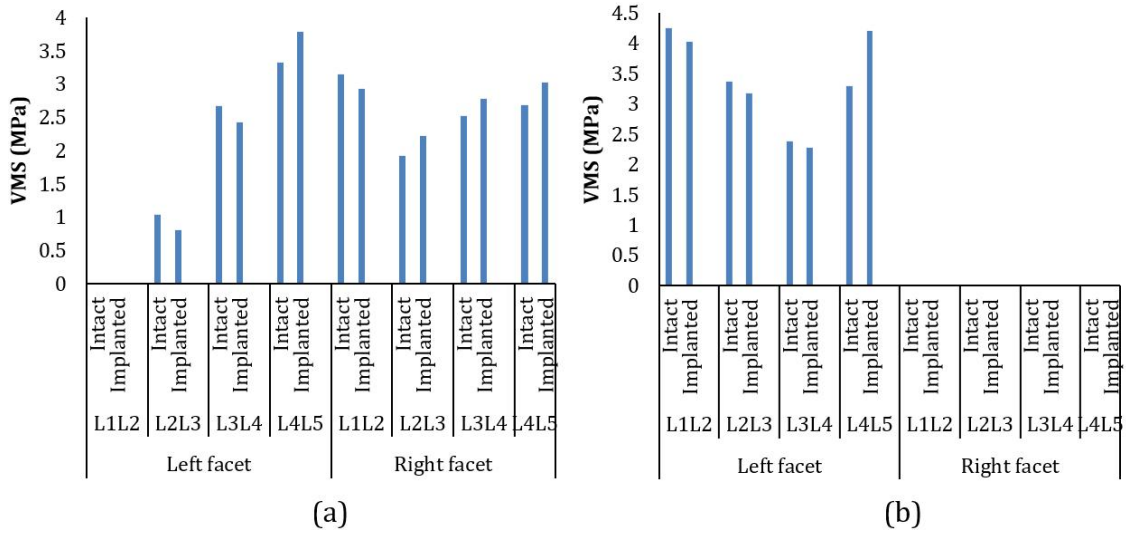

Figure 9. Facet stress in the lumbar spine between the intact and implanted lumbar spine in (a) left bending motion, (b) right torsion motion.

The findings of this study indicated that the facet stress values increased at the treated level of L4L5 after Prodisc-L implantation ranging from 12% to 27% of differences. Previous FE model studies also indicated similar findings with the present study [4], [10], [36], [37]. This is due to the facet load stress was transmitted from the adjacent level of implanted to the treated level during lumbar spine motions. In torsion motion, for example, while facet stresses for L1L2, L2L3, and L3L4 decreased, facet stresses at the treated level of L4L5 increased significantly. This phenomenon was caused by the load transmitted to the lower side of superior and inferior facet at the treated level [34].

Moreover, several FE studies have suggested that lumbar TDR using ball and socket type of artificial disc such as Prodisc-L results in increased facet loading at the surgical level and most significant during lateral bending and torsion [36], [38], [39]. This is due to the fact that the degree of lumbar artificial disc restriction affects post-implantation kinematics and load transfer, so that a semi-constrained artificial disc, such as Prodisc-L, results in the facets being partially loaded when compared to an unconstrained prosthesis [10], [34], [35].

4. CONCLUSION

This study has investigated the effects of TDR prosthesis on the spinal facet joint on the ROM and facet stress at the lumbar spine region in flexion, extension, left bending, and right torsion motions using FE method. The implanted spine increased the ROM during flexion-extension motion and left bending motion. It also increased the facet stresses in all spine motions, particularly at the treated level of L4L5 after TDR. In the context of long-term effects, this could be one of the potential causes of early facet arthrosis, facet degeneration, and reoccurrence lower back pain in the immediate future.

ACKNOWLEDGEMENT

The works was supported by the Universiti Teknikal Malaysia Melaka (UTeM) and funded by the Ministry of Higher Education Malaysia (ERGS/2012/FKM/TK01/02/3/E00005).

REFERENCES

[1] C. Schätz, K. Ritter-Lang, L. Gössel, and N. Dreßler. Comparison of Single-Level and Multiple-Level Outcomes of Total Disc Arthroplasty: 24-Month Results. *Int. J. Spine Surg.*, vol. **9**, (2015) pp.177-190.

[2] J. Alex Sielatycki M.D. , Clinton J. Devin M.D. , Jacquelyn Pennings , Marissa Koscielski M.S. A novel lumbar total joint replacement may be an improvement over fusion for degenerative lumbar conditions: a comparative analysis of patient-reported outcomes at 1 year. *Spine J.*, (2020).

[3] Formica, C., Zanirato, A., Divano, S., Basso, M., Cavagnaro, L., Alessio Mazzola, M. Total disc replacement for lumbar degenerative disc disease: single centre 20 years experience, European Spine Journal, **29**(7), (2020) pp.1518–1526.

[4] A. Younus, A. Kelly, and W. van der Meulen, Motion preservation after cervical total disc replacement surgery-fact or fiction?, *Interdiscip. Neurosurg. Adv. Tech. Case Manag.*, vol. **23**, (2021), pp.100965.

[5] J. Choi, D. A. Shin, and S. Kim, Biomechanical effects of the geometry of ball-and-socket artificial disc on lumbar spine, *Spine (Phila. Pa. 1976).*, vol. **42**, no. 6, (2017) pp.E332–E339.

[6] Zigler, J., Delamarter, R., Spivak, J. M., Linovitz, R. J., Danielson, G. O., Haider, T. T. Results of the Prospective , Randomized , Multicenter Food and Drug Administration Investigational Device Exemption Study of the ProDisc -L Total Disc Replacement Versus Circumferential Fusion for the Treatment of 1-Level Degenerative Disc Disease," vol. **32**, no. 11, (2007) pp.1155–1162.

[7] C. Park, K. Ryu, K. Lee, and H. Lee, Clinical Outcome of Lumbar Total Disc, vol. **37**, no. 8, (2012) pp.672–677.

[8] T. S. Yoon, A. J. Greenberg, P. V. Mummaneni, and W. J. Shi, Risk Factors of Extended Hospital Stay After One-Level Anterior Cervical Discectomy Fusion or Disc Replacement: Results from 1004 Patients in Food and Drug Administration Trials, *World Neurosurg.*, vol. **145**, no. September, (2021) pp.e7–e13.

[9] A. Rohlmann, T. Zander, M. Rao, and G. Bergmann, Realistic loading conditions for upper body bending, *J. Biomech.*, vol. **42**, no. 7, (2009) pp.884–890.

[10] T. Zander, A. Rohlmann, G. Bergmann, and E. Al, Influence of different artificial disc kinematics on spine biomechanics, *Clin. Biomech.*, vol. **24**, no. 2, (2009) pp.135–142.

[11] U. K. Chang, D. H. Kim, M. C. Lee, R. Willenberg, S. H. Kim, and J. Lim, Changes in adjacent-level disc pressure and facet joint force after cervical arthroplasty compared with cervical discectomy and fusion, *J. Neurosurg. Spine*, vol. **7**, no. 1, (2007) pp.33–39.

[12] H. Furunes *et al.*, Facet Arthropathy Following Disc Replacement Versus Rehabilitation: A Prospective Study With 8-Year Follow-Up, *Spine (Phila. Pa. 1976).*, vol. **45**, no. 21, (2020) pp.1467–1475.

[13] V. Moramarco, A. Perez Del Palomar, C. Pappalettere, and M. Doblare, An accurate validation of a computational model of a human lumbosacral segment, *J. Biomech.*, vol. **43**, no. 2, (2010) pp.334-342 NP–9.

[14] J. Kitzen *et al.*, Subsidence after total lumbar disc replacement is predictable and related to clinical outcome, *Eur. Spine J.*, vol. **29**, no. 7, (2020) pp.1544–1552.

[15] H. J. Kim, K. T. Kang, B. S. Chang, C. K. Lee, J. W. Kim, and J. S. Yeom, Biomechanical analysis of fusion segment rigidity upon stress at both the fusion and adjacent segments - A comparison between unilateral and bilateral pedicle screw fixation, *Yonsei Med. J.*, vol. **55**, no. 5, (2014) pp.1386–1394.

[16] S. N. Zahari *et al.*, The Effects of Physiological Biomechanical Loading on Intradiscal Pressure and Annulus Stress in Lumbar Spine : A Finite Element Analysis," vol. 2017,

(2017).
[17] F. Somovilla-Gómez, R. Lostado-Lorza, M. Corral-Bobadilla, and R. Escribano-García, *Improvement in determining the risk of damage to the human lumbar functional spinal unit considering age, height, weight and sex using a combination of FEM and RSM*, vol. **19**, no. 1. Springer Berlin Heidelberg, (2020).
[18] W. M. Park, K. Kim, Y. H. Kim, and E. Al, "Effects of degenerated intervertebral discs on intersegmental rotations, intradiscal pressures, and facet joint forces of the whole lumbar spine," *Comput. Biol. Med.*, vol. **43**, no. 9, (2013) pp.1234–1240.
[19] H. M. Afify, M. S. Mabrouk, and S. Y. Marzouk, Comparative Biomechanical Analysis of Lumbar Disc Arthroplasty using Finite Element Modeling, in *2018 13th International Conference on Computer Engineering and Systems (ICCES)*, (2018), pp.85–90.
[20] T. Zander, M. Dreischarf, A. K. Timm, W. W. Baumann, and H. Schmidt, Impact of material and morphological parameters on the mechanical response of the lumbar spine – A finite element sensitivity study, *J. Biomech.*, vol. **53**, (2017) pp.185–190.
[21] A. Rohlmann, A. Mann, T. Zander, and G. Bergmann, Effect of an artificial disc on lumbar spine biomechanics: A probabilistic finite element study," *Eur. Spine J.*, vol. **18**, no. 1, (2009) pp.89–97.
[22] S. M. Renner *et al.*, Novel model to analyze the effect of a large compressive follower pre-load on range of motions in a lumbar spine, *J. Biomech.*, vol. **40**, no. 6, (2007) pp.1326–1332.
[23] M. M. Panjabi, T. R. Oxland, I. Yamamoto, and J. J. Crisco, Mechanical Behavior of the Human Lumbar and Lumbosacral Spine as Shown by Three-Dimensional Load-Displacement Curves, *J. Bone Jt. Surg.*, vol. **76**, no. 3, (1994) pp.413–424.
[24] M. Dreischarf, T. Zander, G. Bergmann, and A. Rohlmann, A non-optimized follower load path may cause considerable intervertebral rotations, *J. Biomech.*, vol. **43**, no. 13, (2010) pp.2625–2628.
[25] C. Sköld, H. Tropp, S. Berg, and E. Al, Five-year follow-up of total disc replacement compared to fusion: A randomized controlled trial," *Eur. Spine J.*, vol. **22**, no. 10, (2013) pp.2288–2295.
[26] E. T. Maas *et al.*, Systematic review of patient history and physical examination to diagnose chronic low back pain originating from the facet joints, *Eur. J. Pain (United Kingdom)*, vol. **21**, no. 3, (2017) pp.403–414.
[27] L. Marchi, L. Oliveira, E. Coutinho, and L. Pimenta, The importance of the anterior longitudinal ligament in lumbar disc arthroplasty: 36-Month follow-up experience in extreme lateral total disc replacement, *Int. J. Spine Surg.*, vol. **6**, no. 1, (2012) pp.18–23.
[28] N. B. Bonnheim and T. M. Keaveny, Load-transfer in the human vertebral body following lumbar total disc arthroplasty: Effects of implant size and stiffness in axial compression and forward flexion, *Jor Spine*, vol. **3**, no. 1, (2020) pp.1–10.
[29] P. W. Hitchon *et al.*, Biomechanical studies of an artificial disc implant in the human cadaveric spine, *J. Neurosurg. Spine*, vol. **2**, no. 3, (2005) pp.339–343.
[30] A. Rohlmann, T. Zander, H. Schmidt, H. J. Wilke, and G. Bergmann, Analysis of the influence of disc degeneration on the mechanical behaviour of a lumbar motion segment using the finite element method, *J. Biomech.*, vol. **39**, no. 13, (2006) pp.2484–2490.
[31] M. Dreischarf, A. Shirazi-Adl, N. Arjmand, A. Rohlmann, and H. Schmidt, Estimation of loads on human lumbar spine: A review of in vivo and computational model studies, *J. Biomech.*, vol. **49**, no. 6, (2016) pp.833–845.
[32] M. S. Caicedo, E. Solver, L. Coleman, J. J. Jacobs, and N. J. Hallab, Females with unexplained joint pain following total joint arthroplasty exhibit a higher rate and severity of hypersensitivity to implant metals compared with males: Implications of sex-based bioreactivity differences, *J. Bone Jt. Surg. - Am. Vol.*, vol. **99**, no. 8, (2017) pp.621–628.
[33] D. H. Kim, K. S. Ryu, M. K. Kim, and C. K. Park, Factors influencing segmental range of motion after lumbar total disc replacement using the ProDisc II prosthesis, *J. Neurosurg. Spine*, vol. **7**, no. 2, (2007) pp.131–138.

[34] S. Botolin *et al.*, Facet joint biomechanics at the treated and adjacent levels after total disc replacement, *Spine (Phila. Pa. 1976).*, vol. **36**, no. 1, (2011) p. S92.
[35] T. Takigawa *et al.*, Spinal kinematics and facet load transmission after total disc replacement, *Spine (Phila. Pa. 1976).*, vol. **35**, no. 22, (2010) pp.1160–1166.
[36] S. A. Rundell, J. D. Auerbach, R. A. Balderston, and S. M. Kurtz, Total disc replacement positioning affects facet contact forces and vertebral body strains, *Spine (Phila. Pa. 1976).*, vol. **33**, no. 23, (2008) pp.2510–2517.
[37] F. M. Phillips *et al.*, Effect of two-level total disc replacement on cervical spine kinematics, *Spine (Phila. Pa. 1976).*, vol. **34**, no. 22, (2009) pp.794–799.
[38] K. T. Kim, S. H. Lee, K. S. Suk, J. H. Lee, and B. O. Jeong, Biomechanical changes of the lumbar segment after total disc replacement: Charite®, prodisc®and maverick®using finite element model study, *J. Korean Neurosurg. Soc.*, vol. **47**, no. 6, (2010) pp.446–453.
[39] S. A. Rundell, J. S. Day, J. Isaza, S. Guillory, and S. M. Kurtz, Lumbar total disc replacement impingement sensitivity to disc height distraction, spinal sagittal orientation, implant position, and implant lordosis, *Spine (Phila. Pa. 1976).*, vol. **37,** no. 10, (2012) p324.